DINAME 2019 - Proceedings of the XVIII International Symposium on Dynamic Problems of Mechanics,
M.A. Savi, T.G. Ritto and W.M. Bessa (Editors), ABCM, Buzios, RJ, Brazil, March 10th to 15th, 2019

Mathematical model and validation of the axial dynamics of a vibration-assisted drilling tool

d'Almeida E.F.V.[1], **Aguiar R.R.**[2], **and Ritto T.G.**[1]

[1] Department of Mechanical Engineering - Universidade Federal do Rio de Janeiro, Rio de Janeiro, Brazil

[2] Brazil Technology and Integration Center, Schlumberger Oilfield Services, Rio de Janeiro, Brazil

Abstract: A lumped parameter vibro-impact model is proposed to describe the axial dynamics of a vibration-assisted drilling tool prototype, developed with the objective to improve the drilling efficiency in hard-rock drilling applications. A seven degree-of-freedom mathematical model with four possible impact surfaces is developed to describe the axial vibration dynamics inside this vibration-assisted drilling tool. Field data in high acquisition frequency, measured at multiple location, is used to validate the mathematical model.

Keywords: Vibration-assisted drilling, nonlinear dynamics, model validation, impact

INTRODUCTION

The main focus of this work is to develop a mathematical model which is able to describe the axial dynamics of a vibration assisted drilling tool (VAD). This prototype was submitted to field tests in drilling environment to evaluate and characterize the tool performance. Although the tool has been successfully tested, the level of understanding on the physics of the VAD is limited, as there is no available model to describe the dynamics inside the tool. Thus, a seven degree-of-freedom mathematical model with four possible impact surfaces is proposed to describe the axial vibration dynamics inside this vibration-assisted drilling tool. The validation process of this model includes field data in high acquisition frequency measured in multiple locations. Because the focus of this mathematical model is to recreate the tool dynamics, the effect of the lithology and bit-rock interaction on the rate of penetration are not evaluated in this model.

MATHEMATICAL MODELING

The prototype analyzed in this work is sketched in Fig. 1. A seven degrees-of-freedom lumped parameter vibro-impact system is proposed to model the vibration-assisted drilling tool. This model is able to represent the phenomena of interest, and has a low computational cost.

The axial dynamics of the components inside the vibration-assisted drilling tool can be simplified into the impact interaction between four main components: the tool housing, anvil, recoil spring and bit assembly, as indicated by Fig. 1. The tool housing is responsible for transmitting the loads from the surface to the bit, as well as isolate the internal components from the drilling mud. The main purpose of the anvil, as the name suggests, is to work as an impacting mass. The recoil spring functions as an energy storage mechanism. Finally, the bit assembly is responsible for transmitting the impact loads to the rock formation, as the drill bit is a sub-component of this assembly. Additionally, the bit assembly contains a measurement sub, which is equipped with a 3-axis accelerometer, with maximum sensor range of 250g and measurement frequency of 1024Hz, that is responsible to record field data close to the drill bit.

Besides these four components, other tools must be considered in the axial dynamics modeling. These tools are: the positive displacement motor (PDM), another measurement sub, the Measurement While Drilling Tool (MWD) and the Logging While Drilling Tool (LWD). The PDM works as an inverted positive displacement pumps, converting the hydraulic power of the mud fluid into mechanical power. The measurement sub is responsible for recording field data above the tool to evaluate the axial vibration propagation through the drill string. The MWD is a responsible for the evaluation of the well path, and transmitting this information in real time by means of a pressure wave (mud pulsing). The LWD measures geologic parameters, such as resistivity and porosity, and stores this downhole data to be evaluated after the tool is retrieved.

The working principle of this prototype can be reduced into five steps. First, an excitation force drives the anvil towards the bit assembly. Next, the anvil makes contact with the bit assembly (impact face), which results in an impact force, transmitted to the rock by the bit assembly. Following, the excitation force pushes the anvil towards the recoil spring. In the fourth step, the anvil impacts the recoil spring, which results in elastic deformation of the spring, converting the kinetic energy of the anvil into elastic potential energy for the next movement cycle. Finally, the spring and the excitation force drives the anvil in the direction of the bit assembly, restarting the cycle.

The equations of motion, as given in Eq. (1), represent the axial displacement of the seven degree-of-freedom model of the vibration-assisted drilling tool. These can be derived by applying the Euler-Lagrange equation to the model rep-

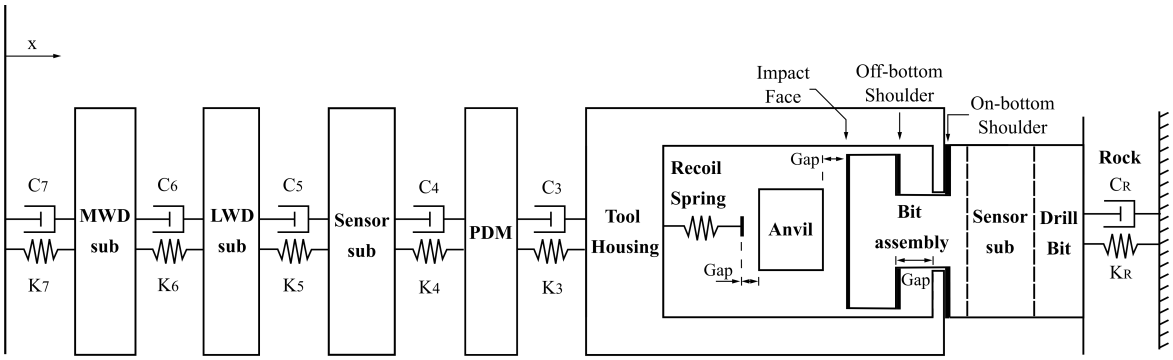

Figure 1: Sketch of the multi-body model for the vibration-assisted drilling tool.

resented in Fig. 1. In this model, the external forces, represented in the parameter $[\mathbf{F}](\mathbf{x},t)$, can be divided into four categories: impact forces, rock interaction force, excitation force and fluid-structure interaction force.

$$[\mathbf{M}]\ddot{\mathbf{x}}(t)+[\mathbf{C}]\dot{\mathbf{x}}(t)+[\mathbf{K}]\mathbf{x}(t)=[\mathbf{F}](\mathbf{x},t) \tag{1}$$

To model the impact dynamics, three impact force models were considered: Hertz model, Spring-dashpot model and Hunt-Crossley model, as explored by Gilardi and Sharf (2002). A local dynamics analysis, as described by Ajibose, Wiercigroch and Pavlovskaia (2010), indicates that, in the case of a one degree-of-freedom drift impact oscillator, all three models result in almost identical dynamic behavior. Thus, as a first approach, the spring-dashpot model is proposed to describe all impact interaction within the system, as given in Eq. (2).

$$F_I = H(\delta)(k_I\delta + c_I\dot{\delta}) \tag{2}$$

where $H(\delta)$ is the Heaviside function, k_I, c_I and δ are, respectively, the stiffness coefficient, viscous damping coefficient and the indentation derived from the spring-dashpot impact model.

The effect of the lithology on the rate of penetration (ROP) is not considered in this model. Hence, the rock formation is modeled only as a flexible support to the entire drill string, not capturing any effect of ROP. To account possible discontinuous behavior (bit-bounce) the equation of the reaction force from the rock follows the same structure applied to the impact models' equations, described by Eq. (3).

$$F_R = H(\delta_R)(k_R\delta_R + c_R\dot{\delta}_R) \tag{3}$$

where k_R, c_R and δ_R are, respectively, the stiffness, viscous damping coefficient and the indentation derived from the impact model applied to the rock formation.

The excitation force that drives the impacting anvil is modeled as a periodic force that considers two major parameters: the mud flow rate and the relative displacement of the anvil in relation to the tool housing, as represented in Eq. (4).

$$F_H = F_o\cos(\alpha Qt+\phi)\sin(\mathscr{F}(x,t)+\psi) \tag{4}$$

where Q is the mud flow rate in revolutions per gallon, $\mathscr{F}(x,t)$ represents the relative displacement between the anvil and the tool housing, α, ϕ and ψ are constants.

Additionally, the vibration-assisted drilling tool housing is filled with a low viscosity fluid to reduce the friction between components. The fluid-structure interaction is simplified as an uniaxial displacement of the anvil the fluid chamber resulting in a drag force, as given by Eq. (5).

$$F_D = c_D(\dot{x}_2)^2 \tag{5}$$

where c_D is the drag coefficient of the low viscosity fluid.

RESULTS

As previously highlighted, the mathematical model should be able to reproduce the main dynamical behavior of the vibration-assisted drilling tool in the series of events observed in the field test data. The tool is submitted to drilling

conditions that emulate an operating drilling environment, which include low weight-on-bit, approximately 4klbf, and constant mud flow rate for a sufficiently long time-frame to achieve steady-state behavior. It is worth mentioning that the field data is recorded by the measurement subs, as both components contains triaxial accelerometers with an acquisition frequency of 1024Hz.

The first result investigates the relationship between the axial vibration peaks and the mud flow rate. The axial vibration peaks are obtained by analyzing the acceleration data in fixed intervals of 200ms to detect the maximum axial vibration peak inside each time window, considering only steady-state data. Next, an investigation of the acceleration data, in the time domain, for each flow rate is required to understand the relationship between the dynamic behavior of the tool and the mud flow rate.

From Fig. 2a, it is possible to analyze and evaluate the average and the dispersion of the axial vibration peaks for each excitation frequency. A summary of the axial vibrations peaks of each event recorded by both measurement subs (above the PDM and close to the drill bit) is represented in Fig. 2a. For a given mud flow rate, each maximum acceleration peak obtained in this analysis is represented as a point in Fig. 2a. The results from the axial vibration data measured close to drill bit seems to indicate a relationship between the axial vibration peak levels and dispersion as a function of the mud flow rate. During the initial stages of the field test, which coincides with the low excitation frequency range (mud flow rate), the axial vibration peaks data reveals high peak amplitudes and relatively low peak dispersion. Next, as the excitation frequency is increased, the system exhibits an increase in the maximum peaks observed. In contrast, there is also a higher dispersion of those peaks, which, as revealed by the both the field data and simulation results, shows a lower average axial vibration peaks than the previous region. This phenomenon ends at higher excitation frequencies, where the peak amplitudes are severely reduced and there is a decrease in acceleration peaks dispersion. The analysis of the axial vibration data of the measurement device located above the PDM reveals that there is a significant reduction in the axial vibrations peaks, when compared to the acceleration data recorded closer to the bit.

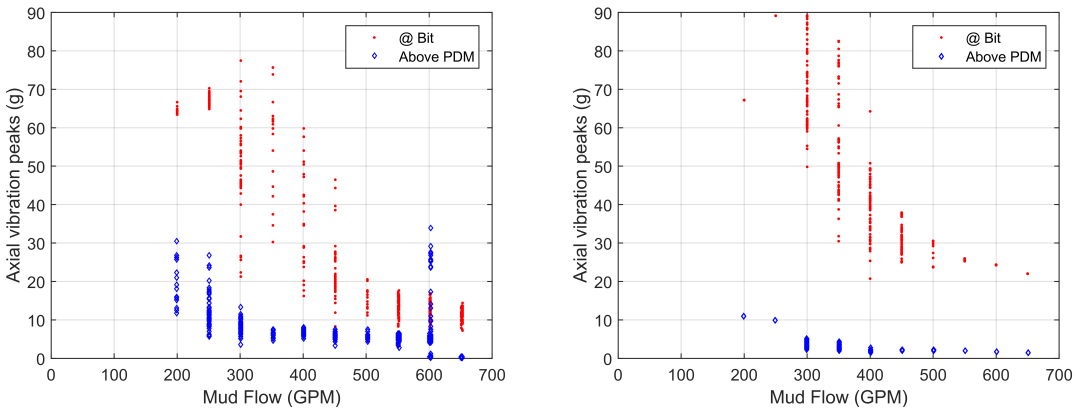

(a) (b)

Figure 2: Axial vibration field data (a) and simulations results (b) of the sensor close to the bit (red dots) and the sensor above the PDM (blue diamonds) obtained in a mud flow sweep scenario from 200 to 650GPM for the prototype.

The simulation results, represented in Fig. 2b, show a good overall match in axial vibration peaks (average and dispersion) when compared with the data measured close to the drill bit recorded in the field test. The mathematical model is also able to recreate the axial vibration peak levels as a function of the mud flow. Furthermore, the increase in dispersion of the axial vibration peaks occurs between 300GPM and 400GPM, which is compatible with the experimental data measured close to the drill bit. The analysis of the axial vibration data of measurement device located above the PDM are in accordance to the field test data, which seems to reveals that, even though the tool is generating high levels of axial vibration close to the drill bit, the effects of these impacts are mitigated by other components of this assembly, reducing the axial vibration levels that are transmitted to the drill pipes located above the assembly.

Although the field data and the simulations results show promising results when analyzing the relationship between the axial vibration peaks and the excitation frequency, a more detailed analysis is required to evaluate the dynamic behavior of the tool and compare with the results of the mathematical model. Thus, an investigation of the acceleration data, in the time domain, for each flow rate is required to understand the relationship between the dynamic behavior and the mud flow rate. In this analysis, three parameters are selected to evaluate the main characteristics of each axial acceleration data: the average axial vibration peaks, the impact frequency and the dynamic behavior.

An analysis of the sensor data close to the bit, given in Fig. 3a, reveals an average axial vibration peak of 65g and an impact frequency of 20Hz. Furthermore, an investigation of the dynamic behavior for each impact cycle seems to indicate

that there are three relevant impacts per cycle. The mathematical model simulations, represented in Fig. 3b, reveal an average axial vibration peak of 67g, an impact frequency of 21Hz and seems to indicate that there are three relevant impacts per cycle. Thus, an evaluation of the simulation results shows a good match with the experimental results, which is already expected since this event corresponds to the calibration event in the validation process.

The validation process also revealed limitations of the mathematical model. The results show a poor match of axial accelerations measured close to the drill bit during high mud high flow rate scenarios. A possible explanation for this phenomenon could be related to the higher influence of system hydraulics, which is not considered in the current dynamic model of the tool. Additionally, the model was not able to match axial accelerations measured above the positive displacement motor, which might be a limitation of this model, as the axial-lateral coupling is not considered.

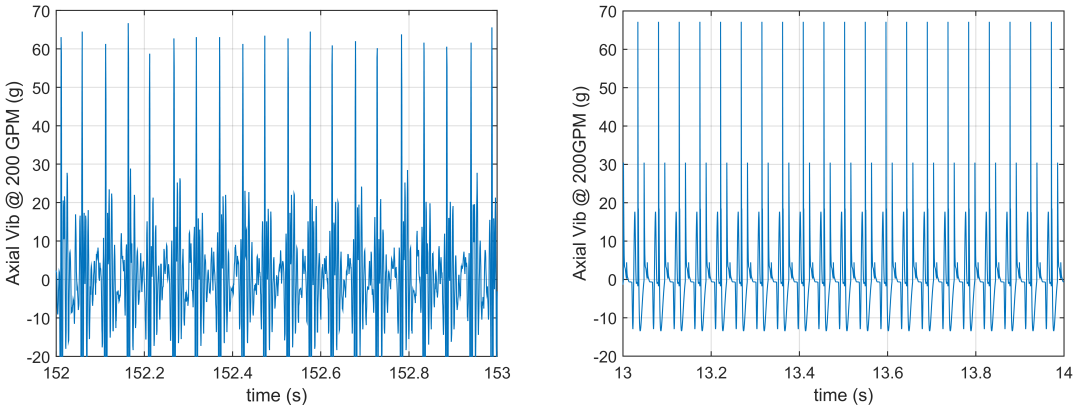

(a) (b)

Figure 3: Axial vibration field data (a) and simulations results (b) in a constant 200GPM mud flow rate scenario during the prototype test.

CONCLUSION

The development of the presented mathematical model focus on the description of the axial vibration dynamics inside a vibration-assisted drilling tool. The validation process of this model included acceleration field data in high acquisition frequency, measured at multiple locations. This dynamic model is composed of a seven degree-of-freedom multi-body system that contains a total of four possible impact surfaces. The analysis of the relationship between the axial vibration peaks and the excitation force frequency reveals that the dynamic model is capable of capturing and reproducing the main dynamic behavior of the vibration-assisted drilling tool observed in the field data. Furthermore, the proposed model is able to reproduce complex dynamic behavior with little computational cost, due to its simplistic dynamic modeling.

ACKNOWLEDGMENTS

The authors would like to acknowledge Schlumberger management for authorizing the publication of this article. The third author would like to acknowledge that this study was financed in part by the *Coordenação de Aperfeiçoamento de Pessoal de Nível Superior* (CAPES) - Finance code 001 - Grant PROEX 803/2018, and the Brazilian agencies: *Conselho Nacional de Desenvolvimento Científico e Tecnológico* (CNPQ) - Grants 303302/2015-1, 400933/2016-0, *Fundação Carlos Chagas Filho de Amparo à Pesquisa do Estado do Rio de Janeiro* (FAPERJ) - Grant E-26/201.572/2014.

REFERENCES

Ajibose, O. K., Wiercigroch, M., Pavlovskaia, E., et al. Global and local dynamics of drifting oscillator for different contact force models, International Journal of Non-Linear Mechanics, v. 45, n. 9, pp. 850858, 2010.

Gilardi, G. and Sharf, I. "Literature survey of contact dynamics modelling." Mechanism and machine theory 37.10 (2002): 1213-1239.

RESPONSIBILITY NOTICE

The authors are the only responsible for the printed material included in this paper.